CR 86084

TM-6-349-260

ELECTRON MICROSCOPE STUDY OF FILM NUCLEATION

BY E. P. MEAGHER

JULY 1968

PREPARED UNDER CONTRACT NO. NAS 12-611 BY

GENERAL DYNAMICS, POMONA DIVISION

POMONA, CALIFORNIA

ELECTRONICS RESEARCH CENTER

NATIONAL AERONAUTICS AND SPACE ADMINISTRATION

TM-6-349-260

ELECTRON MICROSCOPE STUDY OF FILM NUCLEATION

BY E. P. MEAGHER

JULY 1968

PREPARED UNDER CONTRACT NO. NAS 12-611 BY

GENERAL DYNAMICS, POMONA DIVISION

POMONA, CALIFORNIA

ELECTRONICS RESEARCH CENTER

NATIONAL AERONAUTICS AND SPACE ADMINISTRATION

TABLE OF CONTENTS

LIST OF FIGURES

FOREWORD

This report summarizes the progress achieved under Contract NAS 12-611 up to the discontinuance of the work brought about by the voluntary termination of the principal investigator, Dr. E. P. Meagher

INTRODUCTION

The primary objective of the completed phase of this investigation has been to observe the nucleation and growth of iron and vanadium thin films inside an electron microscope and to identify a possible body centered cubic (b.c.c.) to face centered cubic (f.c.c.) polymorphic transformation as a function of deposited mass per unit area. The fact that f.c.c. polymorphs of normally b.c.c. elements exist in thin film has been reported by several investigators. Bublik and Pines (Ref. 1) have reported the occurrence of f.c.c. vanadium films 60-70 Å in thickness while the normal b.c.c. form was observed in films approximately 100 Å thick. More recently, Denbigh and Marcus (Ref. 2) have grown thin film f.c.c. polymorphs of molybdenum and tantalum and Chopra et al. (Ref. 3) have reported the occurrence of f.c.c. molybdenum, tantalum and tungsten.

The in-situ evaporation unit used in this investigation has been previously described in detail (Ref. 4). For completeness, a brief summary description will be included in this report. The basic design of the unit was originally patterned after that developed by Poppa (Ref. 5). In the course of this phase of the investigation additional improvements have been made in the system, particularly in evaporation rate and thickness control.

EXPERIMENTAL SETUP

Electron Microscope

A Hitachi Electron Microscope Model HU-11A was used for the in-situ evaporations. This model is a 100 KV accelerating electron microscope with a double condensing lens system. The microscope is equipped with an image intensifier and a third diffusion pump.

Platinum Grid Heater

The substrate holder consists of a platinum grid which is supported between two 0.030 inch platinum wires (Figure 1). The grid itself is 0.001 inch thick and has three rows of 85 μ holes drilled in it. Pt-PtRh thermocouple wires 0.0005 inch in diameter are spot welded to the grid as shown in Figure 1.

The entire substrate holder assembly is encapsulated in a liquid nitrogen cooled casing to promote cryogenic pumping in the direct vicinity of the grid. This unit is placed in the microscope column on the modified objective pole piece as shown in Figure 2.

Source Heater

Direct current, resistance heated, tungsten or molybdenum baskets are used as source heaters. Provisions have been made for placing two source heaters in the microscope within a tantalum shielding. The holder for the basket and shielding is water cooled.

High purity source materials are melted onto the baskets in a separate vacuum system and the source heater arrangement is then placed in the microscope. One advantage of having two source heaters in the microscope is to permit evaporation of a fresh substrate surface just prior to evaporating the material to be studied.

Substrate Preparation

Carbon or silicon monoxide films are evaporated onto clean glass slides upon which a thin layer of victawet has been previously deposited. The films, which are approximately 300 A thick, are then floated off the glass slides by immersing the slides in distilled water and a small fragment of the film is then placed on the platinum grid over the rows of 85 μ holes.

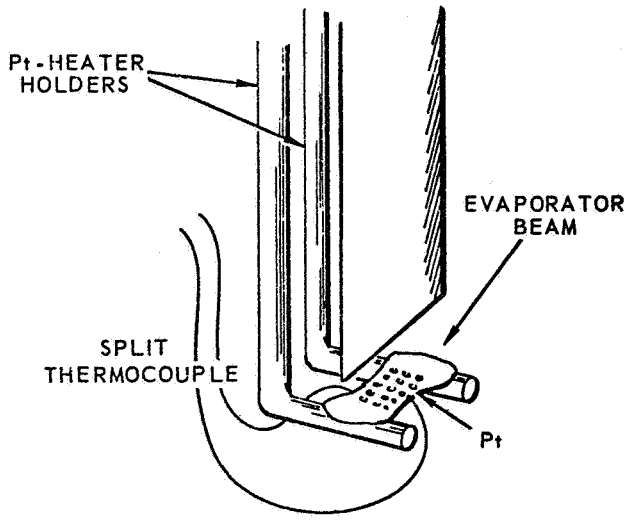

Figure 1. Open Substrate.

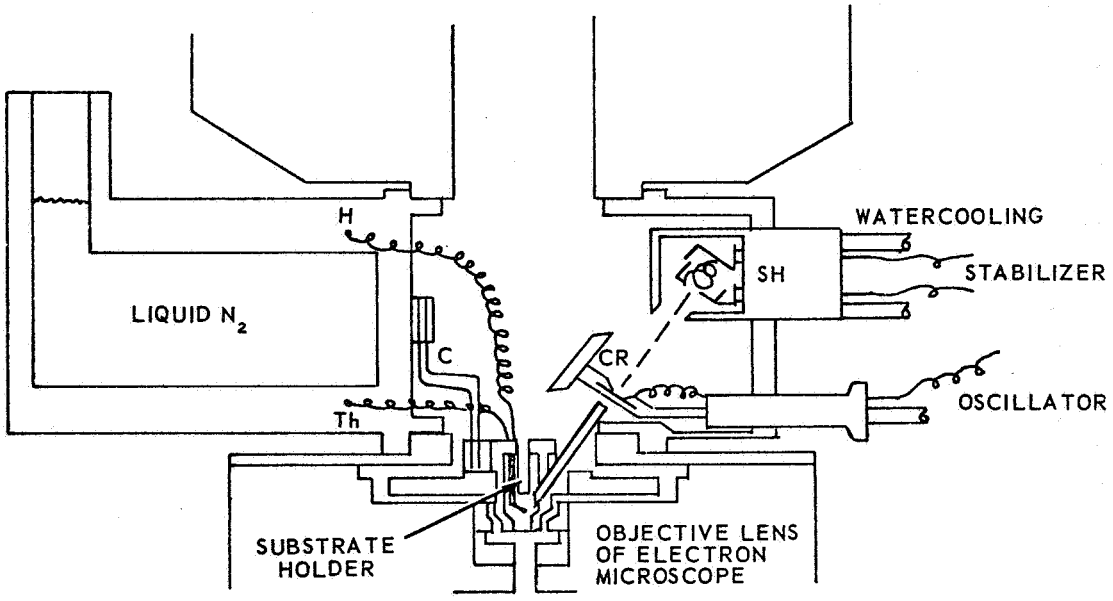

H = HEATER TERMINAL FOR SUBSTRATE; C = COOLING CONDUCTOR
TH = THERMOCOUPLE TERMINAL, CR = CRYSTAL MONITOR – SHUTTER
SH = SOURCE HEATER ARRANGEMENT

Figure 2. Cross Section Through In-Situ Deposition Equipment.

Substrate Temperature

The substrate is resistance heated by passing a direct current through the platinum grid. A somewhat unique technique is required to measure the temperature of the grid due to the fact that a voltage drop is created at the thermocouple joint due to the heating current passing thru the grid. This interferes with the thermovoltage reading one normally makes with a potentiometer. To overcome this problem, the temperature of the grid is determined by interrupting the heating current and plotting the thermovoltage (of the cooling curve) on a high speed recorder. By extrapolation of the voltage curve to the instant of current cut-off, the operating temperature of the grid can be defined.

Rate Monitoring

Rate control of the in-situ evaporation is of the utmost importance for a detailed study of the nucleation and growth of thin films. Recent improvements of the in-situ evaporation system have made it possible to continuously monitor and control the rate of evaporation as the deposition is carried out. This technique was developed in conjunction with an Air Force Avionics Laboratory Contract AF 33(615)-67-C-1911.

Figure 2 shows the shuttered position of the crystal monitor as the evaporation rate is being established. Once a constant rate has been established, the crystal is pulled back to allow continuous monitoring as the deposition is carried out.

The block diagram in Figure 3 shows the components of the monitoring system. The crystal oscillator frequency is simultaneously printed on a paper tape and plotted versus time on a strip chart recorder. Plotting frequency versus time facilitiates maintaining a particular rate of change of frequency as the deposition proceeds. It has been found in the runs carried out to date that as material is evaporated from the resistance heated source basket the evaporation rate varies and the heating current must be changed accordingly to maintain a constant rate.

Film Thickness Determinations

Determining the film thickness of the in-situ depositions by optical interferometric methods is not entirely satisfactory for two reasons. The carbon film, which is supported on the platinum grid, is not entirely flat when viewed in the electron microscope. The film is wrinkled on a very small scale which causes local variations in the growth rate across the film. Since one is interested only in the growth rate in the region where the in-situ deposition study is made, the film thickness in this area must be determined. This area is usually in the neighborhood of a hundred square microns in extent. Secondly, removal

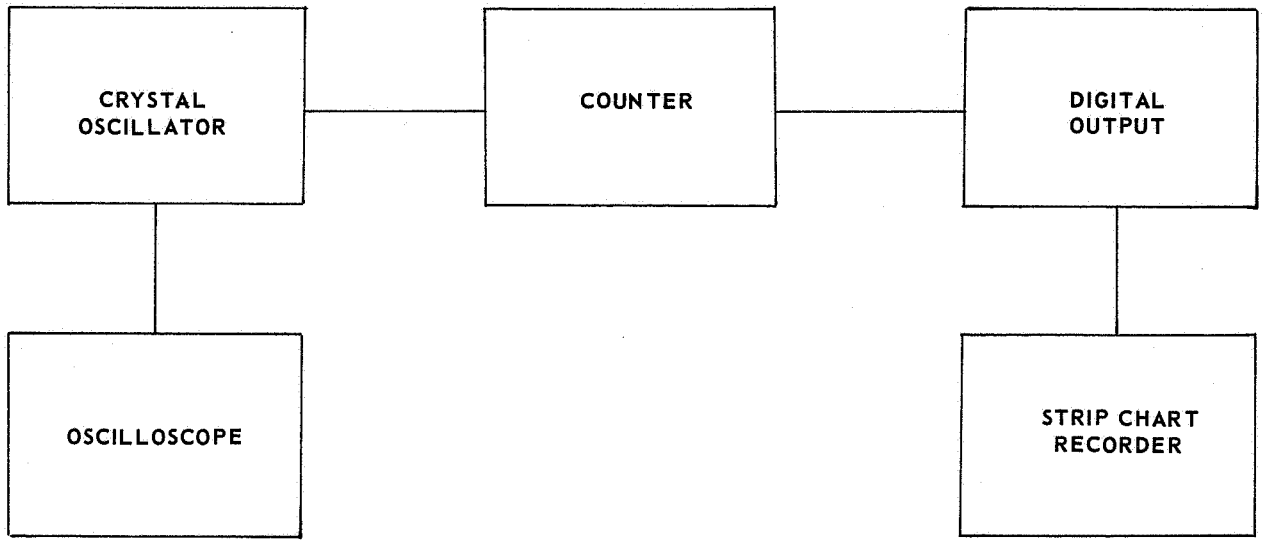

Figure 3. Components of the In-Situ Rate Monitoring System, Block Diagram.

of the evaporated film in sizeable pieces from the platinum grid is difficult after the grid has been heated. This causes problems in obtaining good optical interferometer readings.

An alternative method for the determination of film thicknesses in the electron microscope has been developed for polycrystalline films under the Air Force Avionics Laboratory Contract AF 33(615)-67-C-1911. This same technique has been applied to film thicknesses determinations in this investigation.

Previous investigators have demonstrated that by measuring the decrease in the intensity of an electron beam upon its transmittance through some material, the thickness of that material can be determined (Ref. 2 and 3).

The relation $I_T = I_o e^{-Qt}$ is utilized where:

I_T = intensity of the transmitted beam

I_o = intensity of the direct beam

Q = total scattering constant

t = thickness of the scattering material.

This technique requires that one determine experimentally the value of Q which is characteristic for each type of scattering material. Upon measuring the ratio I_T/I_o one is able to calculate the thickness (t). Measurement of the intensities can be made in arbitrary units since only the ratio I_T/I_o is needed in the determination.

The above relation is applicable only for amorphous materials or for materials whose crystallite size is less than the resolving power of the electron microscope. However, its use may be extended to include randomly oriented polycrystalline materials if one assumes that the loss of transmitted intensity due to diffraction is a function of thickness.

Intensities of the direct and transmitted electron beam are measured with the standard exposure meter supplied with the Hitachi HU-11A Electron Microscope. This system is limited to the detection of electron beam densities between 5×10^{-12} and 1×10^{-10} amps/cm^2. There is, therefore, an upper limit to the thickness of a film which can be measured with this technique. For iron this limit is between 800 and 1000 Å.

Scattering constants for polycrystalline iron and vanadium films were determined by plotting the log (I_T/I_o) versus the thickness of the films. These specimens were deposited in a separate vacuum system on amorphous carbon and their thicknesses determined with an optical interferomter. Intensities were measured, for all cases, with a constant lens setting in the electron microscope. The intensity of the direct beam (I_o) was adjusted to an intensity of 1×10^{-10} amps/cm^2 by allowing the beam to pass through a hole in the carbon substrate. The specimen was then placed in the path of the beam and I_T recorded. The scattering of the carbon is included in this value of I_T and, therefore, must be predetermined.

RESULTS OBTAINED

In-Situ Iron Depositions

The in-situ thin film depositions carried out at various substrate temperatures and growth rates are tabulated in Table I. In all but one experiment, the substrates were amorphous carbon films approximately 300 Å thick. The one exception was an amorphous SiO substrate freshly deposited in-situ on an SiO film just prior to the iron evaporation. The evaporations were carried out at rather low rates in order to observe the presence of phases other than b.c.c. iron during the early stages of growth.

Room Temperature Depositions. - The initial in-situ iron evaporations were carried out on room temperature amorphous-carbon substrates at growth rates of 2, 14 and 20 Å/minute. As the deposition proceeded in each of these runs, the first diffraction rings visible were those with d-spacings of 2.5 and 1.5 Å, respectively. These rings correspond to the two most intense diffraction rings in Fe_3O_4. In the room temperature depositions, the films consisted of either a mixture of b.c.c. Fe and Fe_3O_4 or wholly of Fe_3O_4.

In the 2 and 14 Å/minute depositions only the Fe_3O_4 phase was in evidence. Figure 4 shows the diffraction pattern of the final film in the 14 Å/minute deposition. Following the completion of deposition, the film was slowly heated to approximately 850°C. The diffraction pattern gradually became sharper as the heating proceeded (Figure 5) and random oriented single crystals of Fe_3O_4 grew to diameters as large as 700 Å. No other phases became evident during the annealing procedure.

Figures 6 and 7 are the micrograph and diffraction pattern, respectively, of the 20 Å/minute evaporation. In this deposition a mixture of b.c.c. Fe and Fe_3O_4 was present.

500°C Deposition. - In order to confirm the presence of Fe_3O_4 in the thin film deposits, to observe the effects of a higher substrate temperature on the film growth and to further evaluate the possible presence of other iron phases, a deposition was carried out at an elevated temperature. By increasing the substrate temperature, however, one would presumably enhance the formation of oxide phases.

The film was deposited at a growth rate of approximately 10 Å/minute and within two minutes of the start of the deposition a well developed diffraction pattern was observed. Figures 8 and 9 are the micrograph and diffraction pattern, respectively, of the film following 20 minutes of deposition. The d-spacings and visually estimated relative intensities for the diffraction pattern in Figure 9 are listed in Table II

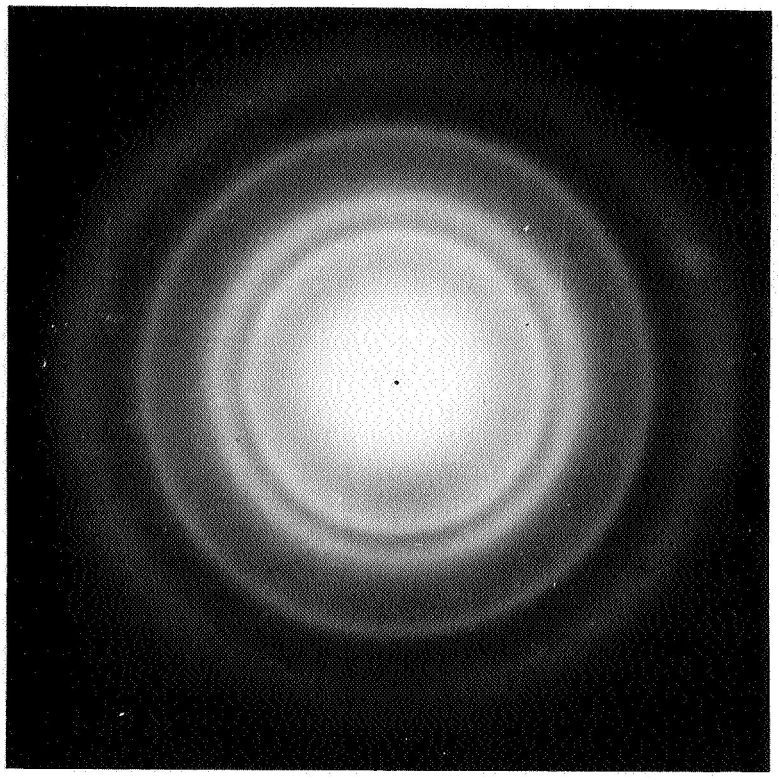

Figure 4. Diffraction Pattern After 14 Minutes Deposition.

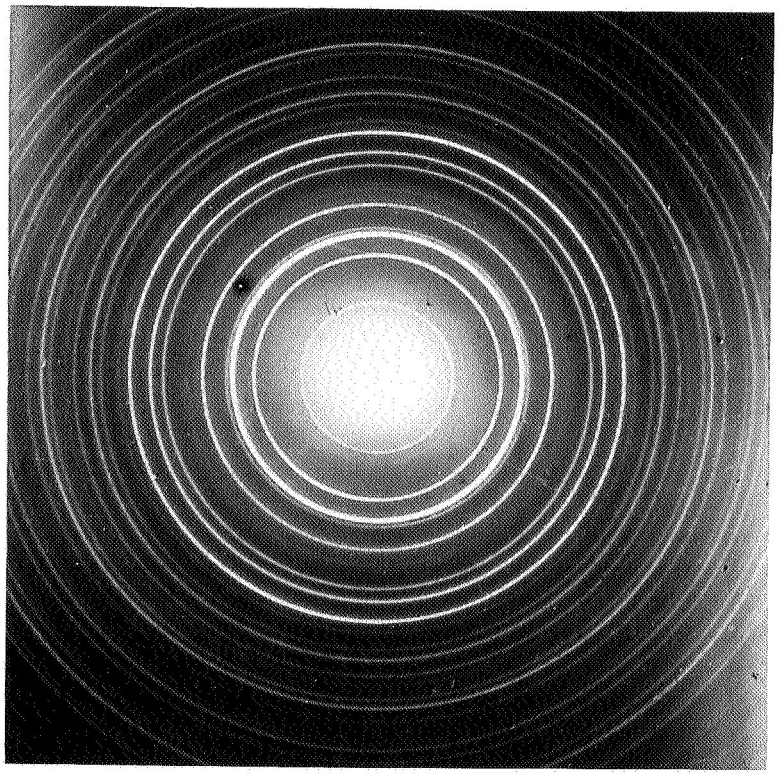

Figure 5. Diffraction Pattern After 850°C Heating.

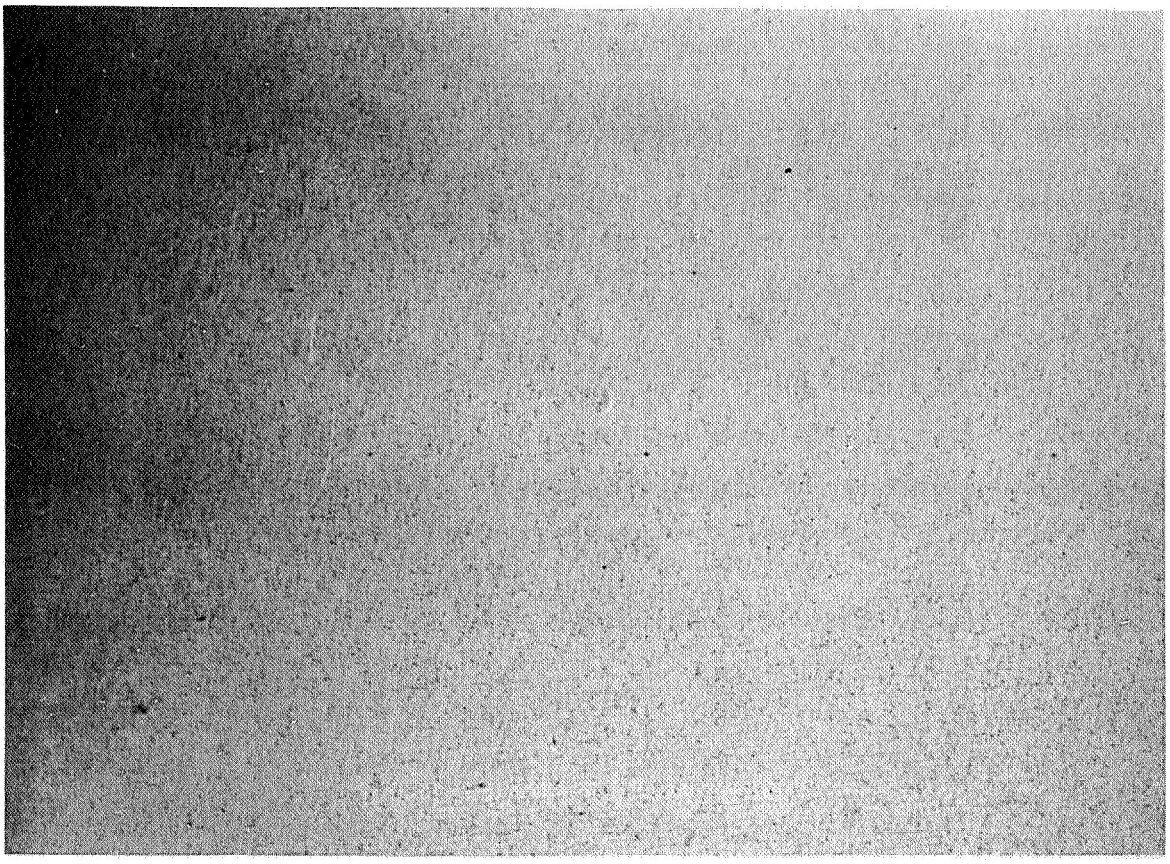

Figure 6. Micrograph Pattern After 20 Å/Minute Evaporation.

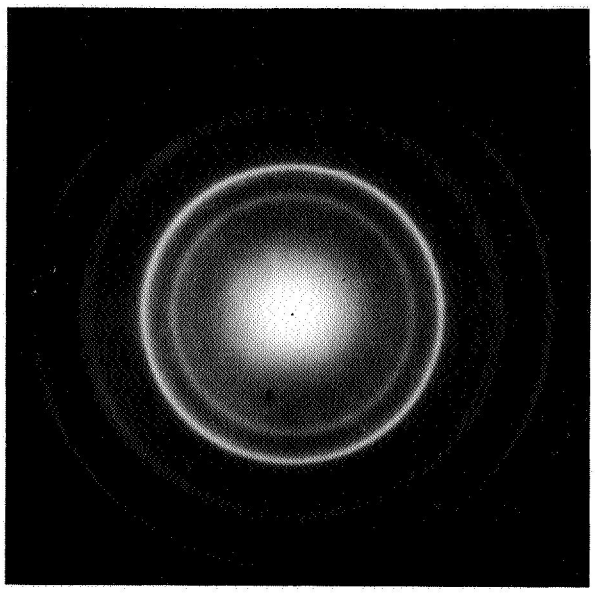

Figure 7. Diffraction Pattern After 20 Å/Minute Evaporation.

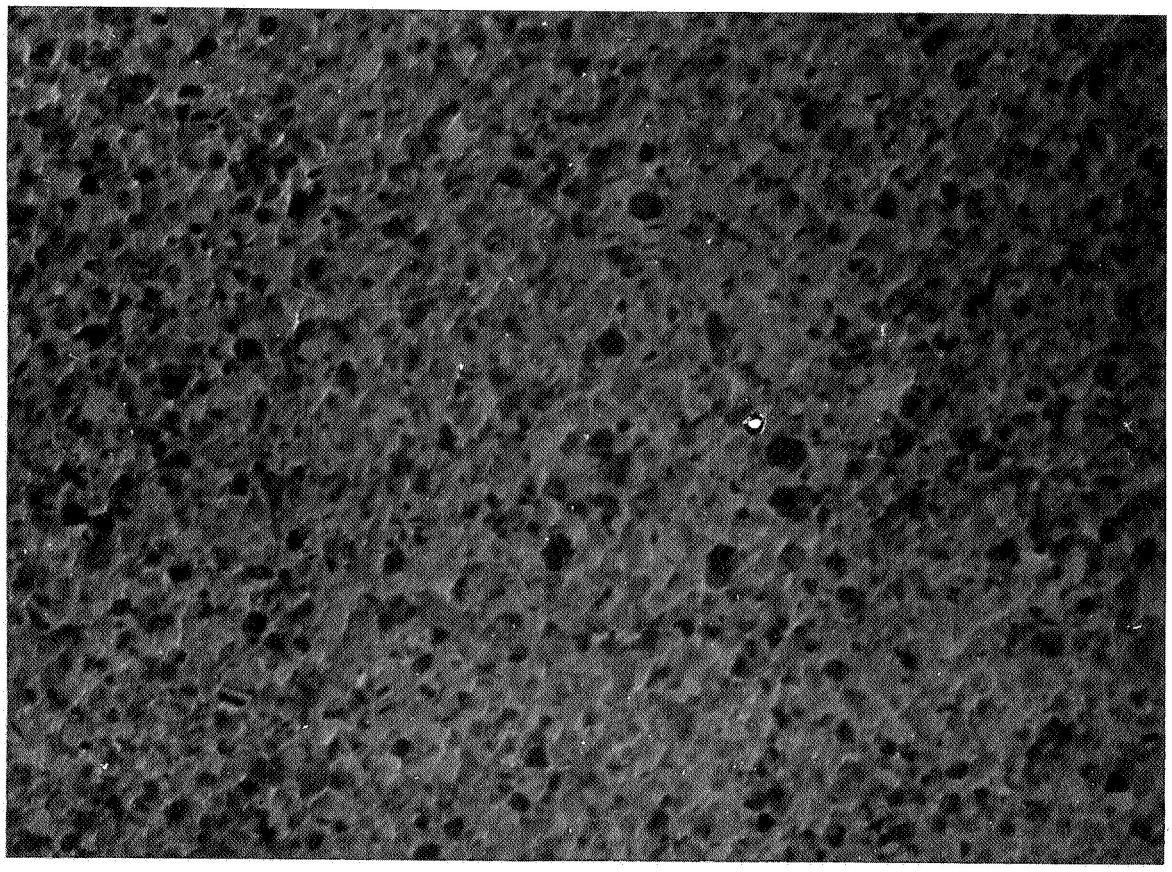

Figure 8. Micrograph Pattern After 20 Minutes of Deposition.

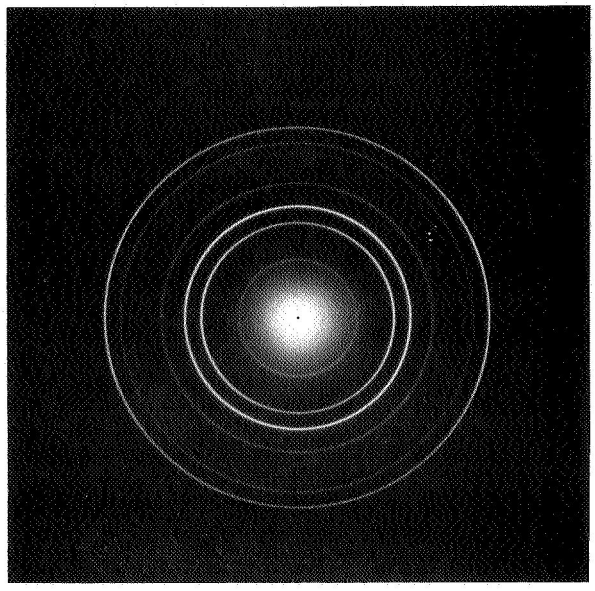

Figure 9. Diffraction Pattern After 20 Minutes of Deposition.

TABLE I

Summary of In-Situ Iron Depositions

Temperature (°C)	Substrate	Growth Rate (Å/minute)	Thickness (Å)	Resulting Film
-50	C	5	150	Fe_3O_4
-50	S10	--	600 - 800	Fe_3O_4
20	C	1-2	100 - 150	Fe_3O_4
20	C	14	150	Fe_3O_4
20	C	20	450	Fe_3O_4 + b.c.c. Fe
500	C	10	200	Fe_3O_4

TABLE II

D-Spacings and Relative Intensities for 500°C Deposition and Fe_3O_4

Fe/C3		Fe_3O_4		
d	I	d	I	hkl
5.00	20	4.85	30	111
4.31	5	4.20	0	200
3.03	80	2.97	60	220
2.57	100	2.53	100	311
2.47	20	2.43	10	222
2.14	40	2.10	50	400
1.97	10	1.93	*	331
1.92	5	1.88	0	420
1.75	30	1.71	40	422
1.65	40	1.62	60	333,511
1.51	80	1.48	70	440
1.45	10	1.42	*	531
1.36	20	1.33	10	620
1.32	30	1.28	30	533
1.29	5	1.27	10	622
1.24	20	1.21	20	444
1.20	10	1.17	*	711,551
1.14	20	1.12	20	642
1.11	30	1.09	50	553,731
1.07	20	1.05	20	800
a_o = 8.6 Å		a_o = 8.39 Å		

*Intensity too weak for detection in x-ray diffraction.

along with the d-spacings and relative x-ray intensities for bulk Fe_3O_4 as tabulated in the ASTM Diffraction Data File. The good agreement between the two patterns suggests that the film is Fe_3O_4. At no time during the deposition was the occurrence of b.c.c. iron evident.

-50°C Depositions. - In all of the room temperature depositions, the initial phase to be nucleated was Fe3O4. Indeed, only the higher rate deposition (20 Å/minute) yielded any free iron at all. Under these conditions the observation of f.c.c. iron would be difficult if it were to occur at all. It is obvious, therefore, that an oxide-free film must be grown in order to study the proposed polymorphic transition. Under the existing vacuum conditions, an attempt was made to inhibit the oxidation of iron at the substrate surface by cooling the substrate to approximately -50°C.

The first iron evaporation carried out under these conditions was on an amorphous carbon substrate. The film was deposited at an approximate growth rate of 5 Å/minute to a final thickness of 150 Å. The resulting film was amorphous in appearance and the diffraction pattern consisted of two broad, diffuse, diffraction rings which possessed d-spacings comparable to the 311 and 440 rings of Fe_3O_4. Annealing of the film resulted in a complete well-developed diffraction pattern of Fe_3O_4 similar to that in Figure 9.

In an attempt to eliminate oxidation of the initial iron deposit on the substrate due to adsorbed oxygen, a second evaporation was carried out at -50°C on a fresh in-situ deposited amorphous silicon monoxide (SiO) substrate. In preparing for the deposition, a SiO film was placed on the platinum grid while crystalline SiO was placed in one tungsten basket and iron was placed in a second basket. Suitable shielding separated the two source heaters in the electron microscope. Upon evaporating a fresh layer of amorphous SiO, the iron source was placed into position and a one minute deposition was made at a rather high rate.

During the above procedure the electron beam was turned off in order to eliminate any effects it may have on the deposition of the film. Following the one minute evaporation, the film was examined and the diffraction pattern revealed a diffuse Fe_3O_4 pattern. Two additional one minute depositions were carried out with an interim examination. The final film consisted wholly of Fe3O4 and was 600 to 800 Å thick.

In-Situ Vanadium Depositions

Two in-situ vanadium depositions have been carried out on amorphous substrates as part of an investigation to ascertain whether a polymorphic transformation (f.c.c. to b.c.c.) occurs as a function of film thickness.

The first in-situ deposition was carried out at room temperature on an amorphous silicon monoxide (SiO) substrate at an approximate growth rate of 6 Å/minute. The resulting film was amorphous in nature as evidenced by micrographs and the diffraction pattern shown in Figure 10.

A second in-situ vanadium deposition was carried out on an amorphous carbon substrate at a temperature of 400°C and a growth rate of approximately 5 Å/minute. This substrate temperature was chosen as a result of the work by Chopra (Ref. 2) who found that at room temperatures sputtered films of normally b.c.c. Ta, Mo and W were amorphous on both amorphous and single crystal substrates. At temperatures between 200° - 400°C a stable f.c.c. modification was observed, whereas; above a substrate temperature of approximately 400°C the normal b.c.c. modification was observed to grow.

Within 2.5 minutes of deposition faint diffraction rings became visible, and after 5.5 minutes two rings with approximate d-spacings 2.45 and 1.45 Å became fairly sharp. These rings continued in intensity and additional rings gradually became visible as the deposition proceeded. Figure 11 is a diffraction pattern recorded upon completion of the deposition. D-spacings and relative intensities of the diffraction pattern have been listed in Table III along with the d-spacings of V_2O_3. It appears quite likely that the deposited film is composed mainly of this oxide of vanadium.

Ex-Situ Vanadium Depositions

In order to determine whether failure to observe f.c.c. vanadium at early stages of in-situ deposit is limited only by environmental problems, a series of ex-situ depositions were carried out in a VHV evaporation system.

This vacuum system is equipped with an electron gun evaporator and an automatic pressure controller. Although a rate monitor is not available in this specific vacuum system, the desired thicknesses were controlled by precalibration with source current.

The depositions were carried out on amorphous carbon films at various temperatures and pressures in an attempt to correlate the growth conditions of the films with the occurrence of oxide phases (Table IV) and to further evaluate the existence of a f.c.c. vanadium polymorph.

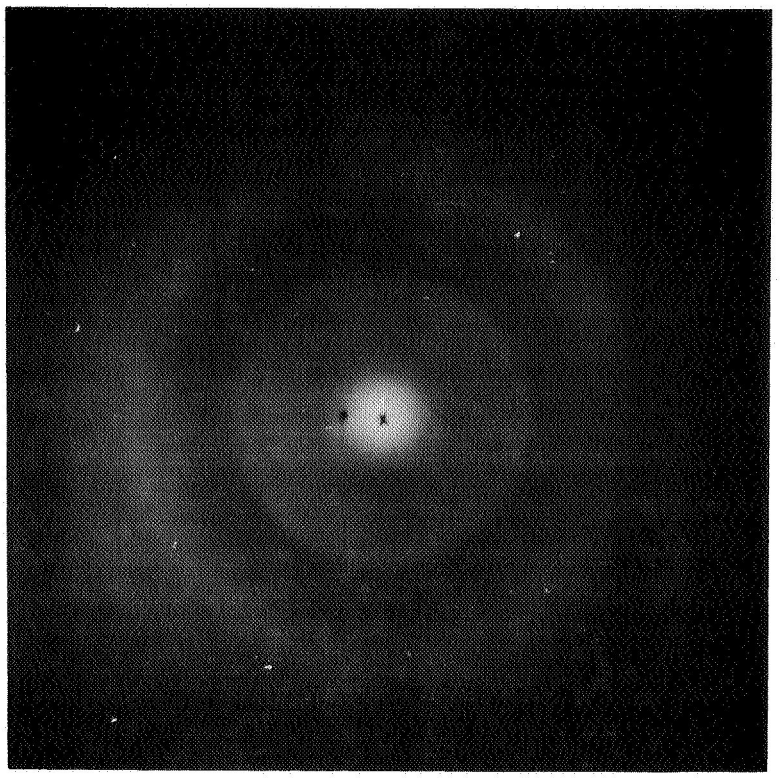

Figure 10. Diffraction Pattern of In-Situ Vanadium Deposition.

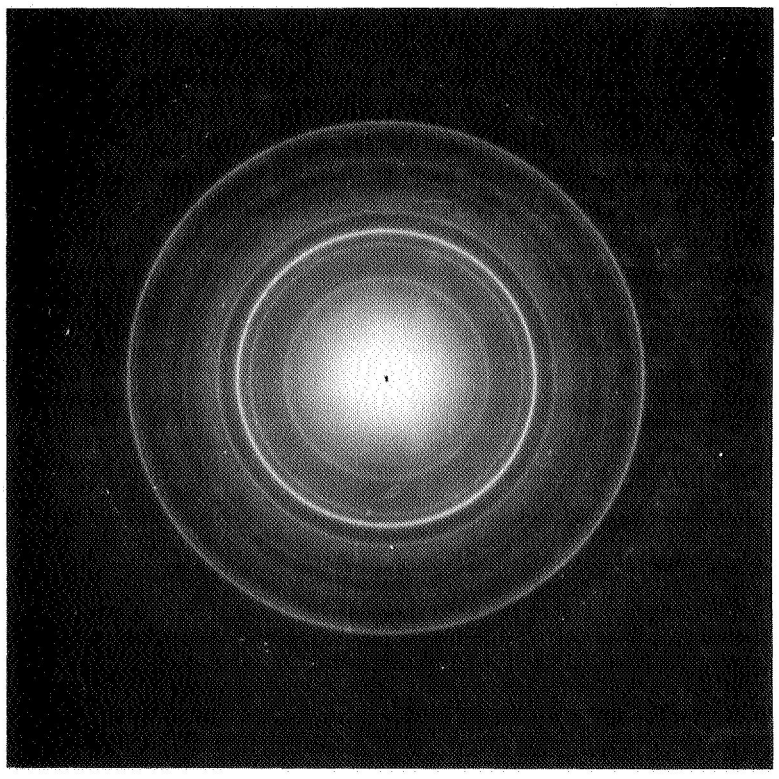

Figure 11. Diffraction Pattern After Completion of the Deposition.

Table III

D-spacings and relative intensities of the 400°C in-situ deposition of vanadium on carbon and V_2O_3.

400°C Deposition V on C					V_2O_3		
d	I				d	I	
3.66	m				3.65	60	
2.72	m.s.				2.70	80	
2.49	v.s.				2.47	60	
2.20	m				2.18	20	
2.01	v.w.				2.03	2	
1.84	m.				1.83	25	
1.71	w						
1.66	m.w.				1.69	100	
1.59	w.				1.57	3	
1.48	m.w.				1.47	25	
1.44	v.s.				1.43	30	
1.28	v.w.				1.33	10	
1.25	w				1.24	4	
1.21	w.				1.22	2	
1.18	v.w.						
1.13	w.						
1.10	w.						
0.96	w.						
0.94	w.						
0.93	w.						
0.91	v.w.						
0.88	m.w.						

TABLE IV

Ex-Situ Vanadium Evaporations

Run #	Temp (^{o}C)	Pressure (torr)	Resulting Film
E331	500	4×10^{-4}	V_2O_3 + ?
E332	250	4×10^{-4}	V_2O_3 + ?
E333	250	1×10^{-5}	b.c.c. V
		7×10^{-7}	b.c.c. V
E334	R.T.	4×10^{-4}	b.c.c. V + VO ?
		1×10^{-5}	b.c.c. V + VO ?

Table IV summarizes the results. At the high substrate temperatures (250°C and 500°C) with a vacuum of 4×10^{-4} torr an oxide phase was observed which has been tentatively identified as V_2O_3 plus an unidentified phase (Figure 12). By increasing the vacuum at 250°C to 1×10^{-5} torr and 7×10^{-5} torr only b.c.c. vanadium was observed.

Of particular interest are the room temperature deposits. The diffraction pattern in Figure 13 represents a film deposited at room temperature and at a pressure of 4×10^{-4} torr. The corresponding deposition at a pressure of 1×10^{-5} torr yielded a similar diffraction pattern. The V_2O_3 phase is not present in the depositions, however, the films cannot be composed solely of b.c.c. vanadium. Table V lists the d-spacings and estimated relative intensities for the diffraction pattern in Figure 13 along with the d-spacings of VO and b.c.c. vanadium. Approximate d-spacings are also listed for a proposed f.c.c. vanadium with an assumed cell edge of 4.06 Å.

Now, vanadium oxide (VO) has been observed (Ref. 6) with a f.c.c. cell of 4.093 Å. It is reported that the composition of this phase can vary from $VO_{0.8}$ (a_o = 4.042) to $VO_{1.2}$ (a_o = 4.126). It can be seen, therefore, that a much better fit can be obtained between the d-spacings of the 4×10^{-4} deposition and VO than that shown in Table V by assuming one of the defect structures. It is difficult to say, therefore, if the 4×10^{-4} deposition represents a VO phase, an f.c.c. vanadium or a mixture of b.c.c. vanadium and the above phases. It is suggested here that caution must be exercised in identifying an f.c.c. vanadium unless it can be shown that the oxide (VO) is not present in the deposition. A more thorough analysis of these room temperature phases is being attempted. As this contract phase is being terminated, this supplementary work, requiring a fairly extensive effort, is carried out separately from this contract.

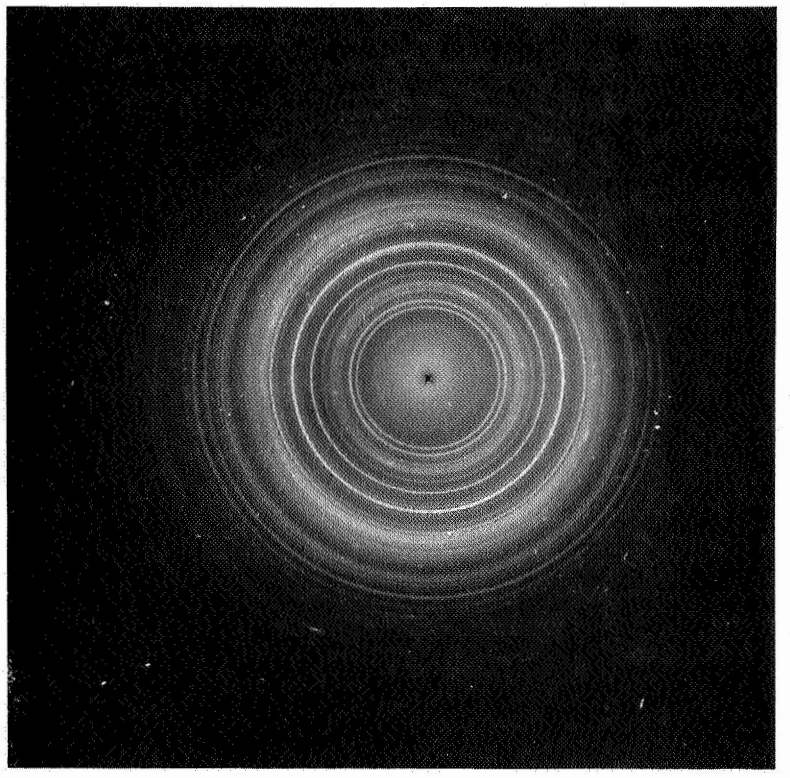

Figure 12. Diffraction Pattern of Ex-Situ Vanadium Evaporations.

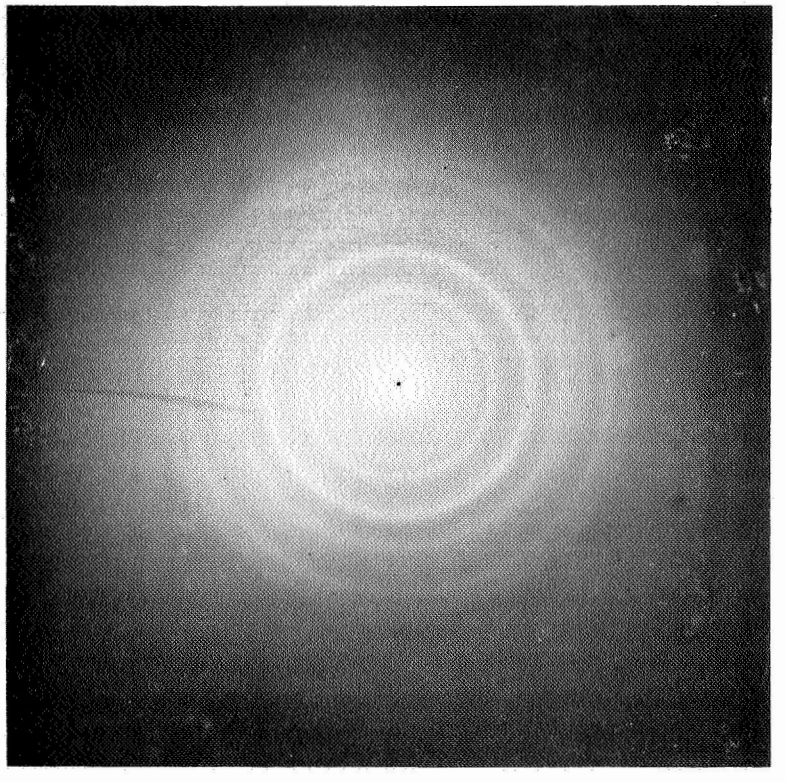

Figure 13. Diffraction Pattern of Ex-Situ Vanadium Evaporations.

TABLE V

D-spacings for the 4×10^{-4} room temperature deposition, b.c.c. Vanadium, V.O. and proposed f.c.c. Vanadium.

4×10^{-4}		b.c.c. V			VO $a_o = 4.09$		fc.c. V $a_o = 4.06$	
d	I	d	I	hkl	d	hkl	d	hkl
2.45	W				2.36	111	2.34	111
2.1	S	2.14	100	110	2.05	200	2.03	200
1.47	S	1.51	7	200	1.45	220	1.44	220
1.20	W	1.238	20	211	1.23	311	1.22	311
0.92	W	0.96	3	310	0.94	331	0.93	331
0.84	W	0.877	3	321				

S = strong

W = weak

CONCLUSIONS

No evidence was established indicating the presence of an f.c.c. phase in either iron or vanadium during the early stages of in-situ film growths. In most cases, the early deposition consisted of a metal oxide phase. Whenever a pure metal phase could be identified, it had b.c.c. structure. The failure to observe an f.c.c. phase, if present, could, of course, be laid to the presence of the oxides. It could be assumed that even if an f.c.c. phase was thermodynamically feasible in a non-oxydizing environment, the presence of the oxide may have prevented its formation. However, this is only conjecture since at the high deposition rate, the b.c.c. phase of iron did form and was clearly identifiable in spite of the presence of Fe_2O_3. From all experiments , in-situ and ex-situ, it is evident that ratio of incident metal particle flux to background pressure governs the presence of a pure metal phase in the early stages of film growth. This is quite indicative of a reactive film growth process. Also, in agreement with such a mechanism is the fact that at higher substrate temperatures the metal flux to pressure ratio must be higher than at low temperatures if oxide formation is to be reduced. By necessity, in-situ deposition must be carried out at very low deposition rates if the early stages of growth are to be reliably observed. As a consequence the vacuum requirements in the electron microscope are quite severe if highly reactive materials such as Fe and Va are to be deposited.

Potentially a most interesting inference can be drawn from the vanadium ex-situ experiments. The room temperature depositions, at a relatively poor vacuum, indicate the formation of either an f.c.c. phase, or, more likely, a mixture of the b.c.c. phase and a vanadium oxide phase (VO). This opens the question whether earlier data on other refractory metal systems could have been subject to the same inherent uncertainty; i.e., whether the presence of diatomic oxides in combination with the b.c.c. phase of the various metals led to erroneous interpretations. As stated earlier, a more thorough analysis of the VO phase is underway and may shed more light on this subject.

REFERENCES

1. Bublik, A. I., and Pines, B. I. A., Dokl. Akad. Nauk, SSSR, 87, page 215, (1952).

2. Chopra, K. L., Randlett, M. R., and Duff, R. H., Phil. Mag., 16, page 261, (1967).

3. Denbigh, P. N., and Marcus, R. B., J. Appl. Phys., 37, page 4325, (1966).

4. Kronenberg, K. J., Final Report of NASA Contract NAS 12-560, (1968).

5. Poppa, H., J. Appl. Phys., 38, page 3883, (1967).

6. Schonberg, Acta Chem. Scandi, 8, p. 221, (1954).